DETECTING AND CHARACTERIZING FRACTURES IN SEDIMENTARY DEPOSITS WITH STONELEY WAVES

Carlos Escandón[1]* and Luis Montes[1]*

[1] Universidad Nacional de Colombia, Bogotá, Colombia
e-mail: escandoncarlos@hotmail.com   lamontesv@unal.edu.co

ABSTRACT

The naturally fractured reservoirs are attractive potential zones for a successful hydrocarbon prospecting, and the variable density logs (VDL) with Chevron patterns generated by Stoneley waves is a suited tool to characterize fractures.

In this project, a simplified algorithm to evaluate fracture location using reflection coefficients and analysis of attenuation was implemented. It also uses a permeability indicator (Stoneley Slowness added by Permeability) to discriminate permeability in fractures.

The algorithm was tested in a foot hill well of the Colombian west range, detecting a previously known fractured sandstone zone and indicating its permeability. Besides, the algorithm detected other existent fractures zones with low permeability for production. Previous well flow evaluation of the localized fractures characterized them as low or no permeability fractures.

Keywords: deposits, fractures, waves, permeability, sonic log, Llanos foothills.

* To whom correspondence may be addressed

RESUMEN

L os yacimientos naturalmente fracturados son atractivos potenciales para la prospección de hidrocar-
buros, y los registros de densidad variable (VDL) con los patrones de flecha generados por las ondas
de Stoneley son una herramienta apropiada para caracterizar fracturas.

En este proyecto se implementó un algoritmo que evalúa directamente la localización de las fracturas en
pared del pozo mediante coeficientes de reflexión y análisis de atenuación de ondas de baja frecuencia tipo
Stoneley, y utiliza la lentitud adicional por permeabilidad de Stoneley como indicador directo de fracturas
para discriminar la existencia de permeabilidad en ellas.

El algoritmo fue probado en un pozo del piedemonte de la Cordillera Oriental Colombiana, en una zona
de arenisca fracturada, donde localizó e indicó la permeabilidad en una zona de fracturas ya conocida y
detectó otras fracturas con permeabilidades poco atractivas para la explotación, las cuales habían mostrado
bajas permeabilidades durante la evaluación de flujo del pozo.

Palabras clave: yacimientos, fracturas, ondas, permeabilidad, registros sónicos, piedemonte llanero.

1. INTRODUCTION

The theory of low and high frequency waves propagating in solids with porous saturated by fluids has been well known from the researches done by Biot (1956), who considered rocks as saturated porous skeletons where viscous fluid moves free along interconnected pores. Including anisotropy and viscoelasticity, (Biot, 1962) the theory has been widely accepted and used as basis for sonic log development and interpretation (Tezuka, Endo, Miyairi, & Brie, 1995; Tezuka & Cheng, 1997), being their predictions confirmed under controlled laboratory conditions (Brown, Batzle, Dey-Sakar, & Peeters, 2000; Wisse, Smeulders, & Dongen, 1998).

Stoneley waves were proposed to measure permeability by Rosenbaum (1974), intending to establish the characteristics of an acoustic logging tool based on the behavior of a pulse emitted in a pit fluid surrounded by a porous formation. It was found that trains of low frequency wave (Tube waves, Stoneley waves) were particularly sensitive to changes in fluid transfer conditions between the formation and the well along its wall (permeability changes). In presence of fractures in the borehole wall the Stoneley waves generate chevron patterns losing energy in permeable zones; phenomena that have successfully used in detecting fractures in calcareous formations; but the technique does not behave appropriately in wells drilling sandstone type formations due to imperfections present in their walls.

Cheng- Chuen and Toksoz (1981) studied the propagation of elastic waves in a fluid-filled borehole with a tool in the center producing synthetic acoustic logs and obtaining the equations that govern the dispersive and reflected Stoneley waves. They also found that the effective radius of the well determines the relative amplitude of the generated modes and concluded that changes in the dispersion characteristics of Stoneley waves are relatively small. A conclusive relationship between permeability and wave attenuation in field data was found (Williams, Zemanek, Angona, Denis & Caldwell, 1984), allowing the development of low frequency tools to detect permeability changes. Paillet and White (1984) predicted the relative excitation of various modes (i.e. guided waves) contained in experimental wave fronts, using a single plane layer

of fluid between two hemi-spaces, providing ve[locity] dispersion curves similar to those presented in [the] wall of a borehole filled with fluid. They also concl[uded] that closer the tool diameter greater the dominanc[e of] the Stoneley mode, indicating the simplest meth[od of] detecting fractures in the borehole wall.

Cheng, Zhang and Burns (1987) related Ston[eley] wave propagation in a cylindrical well along wit[h in] *situ* permeability (Rosenbaum, 1974), founding [that] attenuation and dispersion of the phase velocit[y in]creases when permeability and porosity increase, [and] decrease when frequency increases; they also dete[cted] that the change in the Stoneley wave amplitude is m[ore] sensitive to the change of permeability than to p[hase] velocity change.

Hornby, Johnson, Winkler, & Plumb (1989) i[mple]mented the analysis technique of reflection in pres[ence] of both horizontal and dipping fractures, conside[ring] the aperture of fracture constant along it and as[sum]ing a rigid formation compared with fluid in fract[ure.] In experimental assays they checked the relation[ship] between the magnitude of the reflectivity and the [ap]erture of fracture.

Endo, Ito, Brie, Badri, & El-Sheikh (1997) [as]sessed two wells that crossed a fault, using Ston[eley] waves to evaluate fractures and permeability [and] shear mode for evaluating cross-dipole anisotr[opy.] Comparing the results with image records they [con]cluded that attenuation and Stoneley reflections [are] evidence of open fractures and fault zones. They fo[und] that modeling Stoneley waves allow identify wh[ich] reflections and attenuations are due to irregulari[ties] in the borehole, and also concluded that anisotr[opy] and images integrated with information provide[d by] Stoneley waves offer a better understanding of [frac]tured reservoirs. A series of numerical and analyt[ic] models were developed for use in the interpreta[tion] of Stoneley wave reflections obtained from fract[ures] that intersect the borehole (Kosteck, Jonson, [Ken]neth & Hormby,1998), and also the elasto-dyna[mic] equation that governs tube wave propagation [in a] borehole intercepted by fractures filled with f[luid.] Models for single and double fractures in the p[res]ence of washouts and breakouts were implemente[d by] finite differences. Analytical models were develo[ped] to interpret the Stoneley wave reflections in fract[ured]

in the wall of the borehole, calculating aperture and permeability of the fractures. These models assume a rigid formation, irregularities in the well (washouts, breakouts), changes in lithology, effects of elasticity, single and multiple fractures and the effects of viscosity of fluid. It was determined that a rigid formation model is useless to evaluate fracture parameters because overestimate the value of aperture of fractures.

These techniques were mostly developed for calcareous formations deposits uncommon in Colombia where the presence of borehole wall irregularities in clastic formations could lead to misinterpretation.

A simplified algorithm was created to directly evaluate the location of fractures using a direct permeability indicator to determine the existence of permeability in these fractures. The algorithm was tested on a well, located in the foothill of the Colombian Eastern Cordillera that crosses fractured sandstone zones. It allowed identifying a known fracture zone and assessing its permeability. Besides, the algorithm localized other fractures with permeability unattractive to exploration which showed low permeability during borehole flow tests.

The algorithm is not still able to detect fractures in some cases which have been discerned by other techniques.

2. METHODOLOGY

The implemented MATLAB program follows the next sequence: a) Separation of reflected and transmitted Stoneley waves acquired by the tool by means of a running average filter, using a Hamming window to attenuate edge effects, b) Stacking of reflected and transmitted waves to enhance amplitudes and eliminate non-coherent noise. In the multi-receiver approach a first break picking of direct waves is done, then a linear move out to the 8 signals is applied to finally stack the eight wavelets improving the signal-to-noise ratio. The step is applied both to direct and reflected waves, c) Calculation of the reflection coefficients, d) Estimation of energy in the trace, e) Estimation of attenuation factor Q^{-1} and f) Estimation of Stonely slowness added by permeability. (See Figure 1).
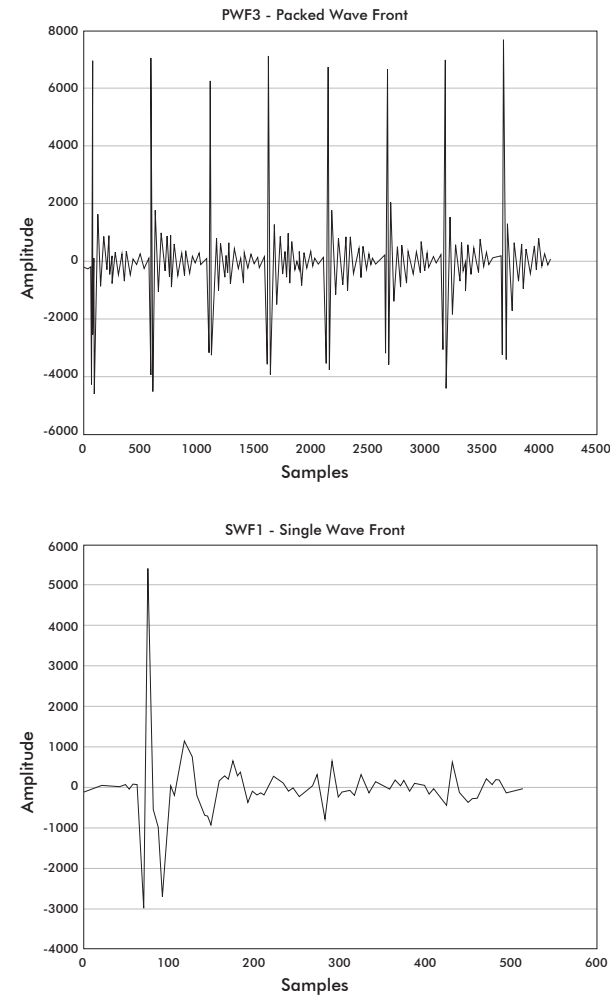

Figure 1 Up, the raw data PWF3 with the eight signals packed, where the first wavelet is the single wavelet SWF1 selected, at bottom

The sequence varies depending on whether the sonic tool has single or multiple receptors with simultaneous processing of Ultrasonic Borehole Imager (UBI) and also of Dipole Shear Sonic Imager (DSI) log. The UBI image processing comprises the orientation and normalization of the image and the equation of amplitudes. A window of 1% of the size of image is used to equalize the color histogram, leaving the image in a single scale. The gross data Packed Waveform PWF3 has eight vectors chained sequentially with the information of eight receptors of the sonic tool, as shown in upper image in Figure 1.

The program was applied to a 600-feet section of an exploration borehole, providing plots of reflection coefficient, energy content in traces, attenuation factor and

Stoneley slowness added by permeability. These plots were correlated along with DSI (Stoneley monopolar mode) and UBI logs for interpretation.

The raw data were acquired with a 51 feet sonic tool working in low frequency Stoneley mode at 600Hz with 40μ second sample rate, providing eight 512-samples wavelets. The tool has $3^{5/8}$ inch diameter and the hole a variable diameter ranging from 5,5 to 21 inch.

Data Structure

The data set includes Ultrasonic Borehole Imager (UBI) to build the well image, Dipole Shear Sonic Imager (DSI) which is the main data to be used by the algorithm, Formation Density Log and Caliper to characterize lithology and imperfections in well´s wall, and Additional Data Logs to perform correlations. All these data are transformed from "dlis" to "las" format and stored as matrixes whose structures are described in the Appendix.

3. PROCESSING SEQUENCE

In the single receptor case, the receiver closest to the source is selected to perform the Stoneley wave analysis, here the first wavelet in the PWF3 (bottom image in Figure 1) corresponds to the SWF1 Wavelet. In multiple receptors case the data set stored contains eight signals as shown in at top image in Figure 1.

Direct and reflected wavelets separation

Through a 20 samples Moving Average filter applied within a standard Hamming window, the direct wave is enhanced whereas the reflected wave is attenuated. In a second step the reflected wave is enhanced by applying first a 30 samples Moving Average filter followed by a single flank Hamming window expressed by the equation:

$$H(k+1) = 0,15 + 0,175\,Cos(\pi(k/n-1)) \qquad (1)$$

Where n is the number of samples and k an integer.

The direct and reflected waves provided by the separation step are depicted in Figure 2, where from the raw data at upper image, the direct wave in the middle and the reflected one at the bottom are observed.
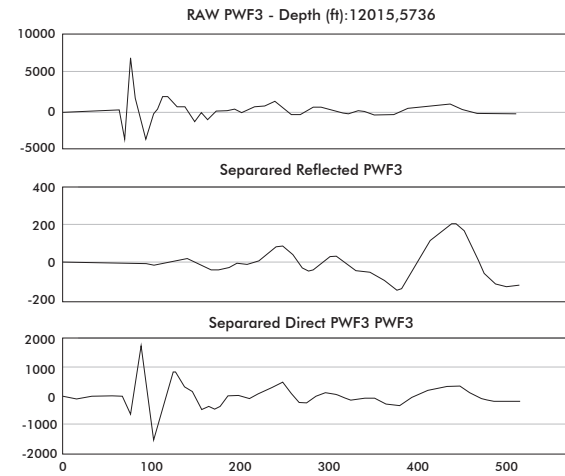

Figure 2 At top the raw wavelet, at the middle the separated direct wave and at the bottom the reflected wavelet after separation

First break picking

The first break picking is performed on the direct wavelet by an automatic procedure. Initially a wavelet transform is applied to establish the limits within which the arrival of the direct wave will be located. This value defines a window where the covariance of the contained samples is calculated. The point where the value of the covariance is strongly deviated from the mean value is considered the first break time. (See Figure 3).
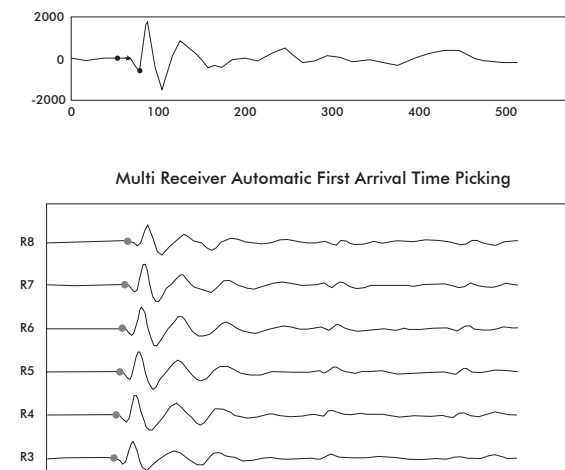

Figure 3 At top, the first break picked is indicated by a dot between the two extreme dots that define the window. Below, first break estimated in multiple receivers

As is known, the Wavelet Transform (WT) captures both frequency and location information (location in time). In order to isolate signal discontinuities, WT uses very short basis functions. At the same time, in order to obtain detailed frequency analysis, WT uses very long basis functions. A way to achieve this is to have short high-frequency basis functions and long low-frequency ones. The wavelet transform decomposed both the directed and reflected wavelet in coefficients at different scales representing low and high frequencies, compressing the signals until they are matched in a time point, which is the upper limit of the window.

The result is shown in Figure 3 where the interval is defined by the two extreme dots whereas the first break time is identified by the dot within the anterior points.

Stacking

This step is applied only in the multiple receptors case. After picked the first break to the eight signals, see bottom image in Figure 3, the slope formed by the eight picked times is calculated and a Linear Move Out (LMO) is applied to finally stack the traces.

Reflection coefficients calculation (RC)

To calculate the reflection coefficients (RC) the Fast Fourier Transform (FFT) is applied separately to the both separated waves, and in the frequency domain the reflection coefficients $RC(\omega)$ are calculated by

$$RC(\omega)=R(\omega)/D(\omega) \qquad (2)$$

$R(\omega)$ and $D(\omega)$ represent the respective reflected and direct waves amplitude spectra. But, because for some frequencies $R(\omega)$ may approaches zero these values are replaced with a function of maximum signal, so *Equation 2* becomes

$$RC(\omega)=(R(\omega)\ D^*(\omega))/(max(D(\omega)\ D^*(\omega),cK)) \qquad (3)$$

Here $D^*(\omega)$ is the transpose of $D(\omega)$, (Hornby *et al.*, 1989). The term provides the maximum peak of the direct wave power spectra and c is a factor, with a value of 1% to guarantee a robust deconvolution. The supplied reflection coefficients series is passed through a Hamming window centered at 600 Hz to taper it in the frequency domain, and the maximum value of these reflection coefficients estimated at a particular depth in the borehole is selected to make a maximum values-depth plot. The

bottom image in Figure 4 shows maximum values estimated since 11 500 to 11 160 feet along the well.

Energy variation calculation (E)

The energy contained in the trace at particular depth (E) is estimated by numerical trapezoidal integration of the area under the power spectra curve providing energy - depth plots. The energy of direct and reflected waves calculated at 12 025 feet of depth in the borehole is observed in the upper image of Figure 4. The maximum reflection coefficient series plotted in depth, estimated in the anterior step, and the energy - depth plots can then be correlated in depth, as observed in bottom image of Figure 4.
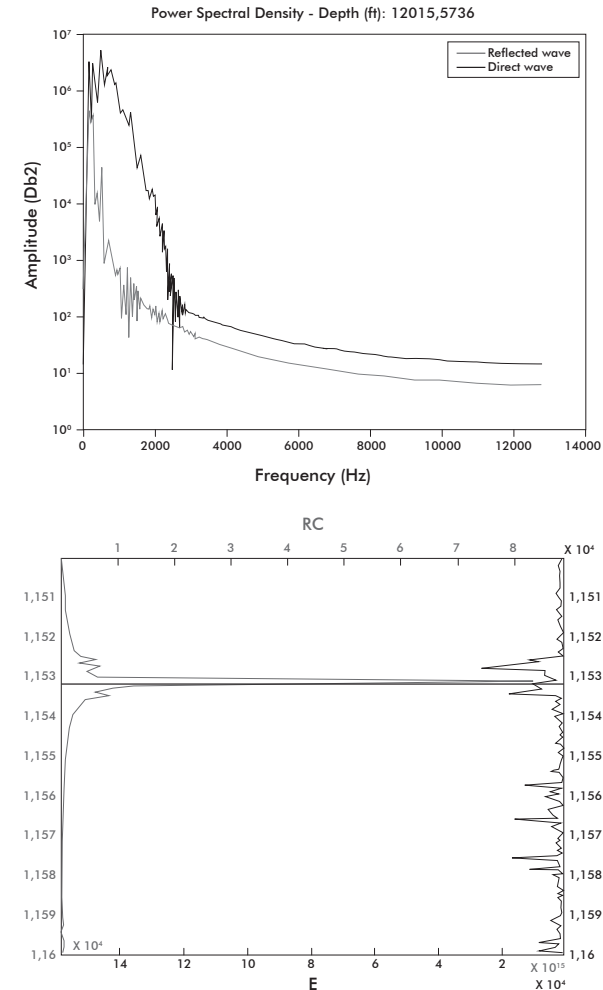

Figure 4 Above, the energy contained in direct and reflected waves at 12 015 feet is plotted and below maximum reflection coefficients (at left) are correlates with energy content (at right)

Q⁻¹ Attenuation estimation

The attenuation of a wave is defined as the loss of energy measured over a period of time, observed as decaying amplitudes along the wavelet, it is mainly caused by the geometrical dispersion and energy absorbed by the medium. Although there are others approaches, to estimate a simplest method was applied. It calculates the ratio of two measured contiguous peak amplitudes separated by one period, according to the following approximation:

$$Q^{-1} \cong \ln\left(U(t)/U(t+\tau)\right) \qquad (4)$$

U(t) is the peak amplitude at time t and *U(t+τ)* is the peak amplitude a period after. In Figure 5 the *Q⁻¹* calculated at different depths since 11 510 to 11 600 feet of the borehole.
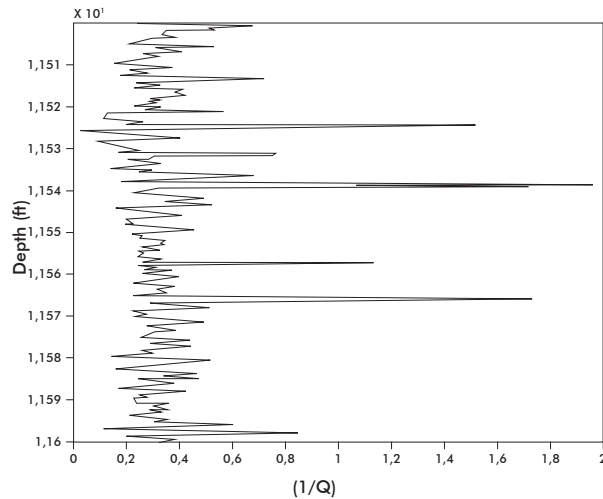

Figure 5 Attenuation factor in depth estimated in the 11 510-11 600 feet interval

Estimation of Stoneley slowness added by permeability

When the Stoneley wave passes from a dry to a permeable area either by porosity or fracturing, the slowness becomes larger and this increment called Stoneley slowness added by permeability is used to estimate and to indicate permeability following the procedure described by Chang, Liu, & Johnson (1988).

In a well of r_b radius within a permeable formation with a matrix shear module G, this indicator can be calculated when the frequency is much lower than Biot's

critical frequency and the wavelength much gre than the well diameter, using:

$$S^2 = \rho_m\left(\frac{1}{K_m}+\frac{1}{G}-\frac{2}{i\omega r_b Z_o}\right)$$

where ρ_m is mud density, K_m volumetric modul the mud, $\omega = 2\pi f$ angular frequency and Z_o, im ance. The successive terms are contribution due to f expansion, expansion of the borehole wall and f movement in pore space.

The impedance is written as:

$$\frac{1}{Z_o} = k_{c2}\,(\kappa/\eta)\frac{H_1^1\left(k_{c2}\,r_b\right)}{H_0^1\left(k_{c2}r_b\right)}$$

H_0^1 and H_1^1 are the zero and one order Hankel f tions respectively, κ is permeability, η is visco and k_{c2} is the Biot's wave number (Biot, 1962.) Stoneley slowness can be expressed (Latifa, Tan Kuijperl, 2001) as:

$$S^2 = S_e^2 + S_p^2$$

S is the measured Stoneley slowness, S_p is Stoneley slowness added by permeability and S_e is Stoneley slowness at zero frequency associated to wave effect in the well and corresponds to the first terms of *Equation 8*. So,

$$S_e^2 = \rho_m\left(\frac{1}{K_m}+\frac{1}{G}\right)$$

Considering that in the DSI tool $S_e \gg S_p$ we ob

$$2S_e(S-S_e) = S_p^2$$

In this way the Stoneley slowness added by meability S_p is calculated as a direct indicato permeability, because represents the additional s ness by the intrusion of the wave in the formatic porous or fractures; this added slowness depend frequency. Figure 6 shows the Stoneley slown added by Permeability calculated between 11 to 11 600 feet of the borehole.
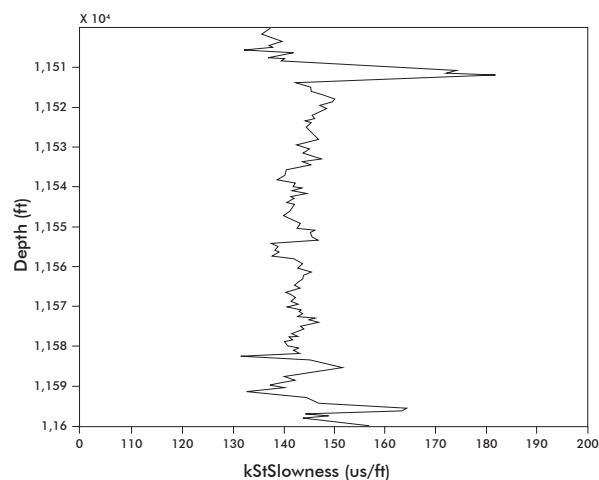
Figure 6 Stoneley slowness added by Permeability calculated along 100 feet of the borehole

4. ANALYSIS OF RESULTS

The program was applied to a studied interval of 600 feet (11 500 to 12 100 feet depth) of an exploratory borehole, where the zones with permeable fractures were plenty identified and characterized. The well data includes DST pressure tests and cores, besides UBI, Gamma ray, Density, porosity, NPHI and DSI logs.

The program provided reflection coefficient, energy content, attenuation factor and Slowness added by permeability series in depth. These results were displayed together with variable density logs (VDL) and UBI images, as shown in Figure 7 with chevron patterns visible along the reflected WF (third image from left).

Table 1 Description of the interval of the studied well

DEPTH	CAL	GR- RHOZ	RC	E	1/Q	StK*	EVENT
12 034	NORMAL	30-2,4	2,5	2,5	0,8	>190	Pack of permeable fractures
12 021	NORMAL	30-2,4	6	8	2 0 5 1	>190	Pack of permeable fractures
12 016	NORMAL	30-2,4	4	6	1,4 0,7 1,4	>190	Permeable fracture
12 009	WIDENED	30-2,4	<1	<2	1,4 0,4 0,9	150	Fractures
12 004	WIDENED	45-2,4	1,8	1	0,7 0,4 0,8	160	Fractures
11 990	NORMAL	45-2,5	0,8	0,2	0,6	<150	Lithological Limit
11 960	NORMAL	52-2,6	1	2,5	0,6	<150	Lithological Limit
11 932	NORMAL	70-2,6	>3	>15	0,5	<150	Fractures
11 926	NORMAL	65-2,5	>3	>15	0,5	<150	Fractures
11 920	NORMAL	50-2,6	2	>10	0,5	<150	Fractures
11 881	WIDENED	>100-2,5	<1	<1	0,5	<150	Lithological Limit
11 860	WIDENED	>400-2,5	<1	<1	0,5	<150	Lithological Limit
11 851	WIDENED	>400-2,5	<1	<1	0,5	<150	Lithological Limit
11 830	WIDENED	180-2,6	<1	<1	0,5	<150	Lithological Limit
11 728	NORMAL	>150-2,6	1,7	2	0,6 0,2 0,8	150	Fractures

Table 1 Description of the interval of the studied well

DEPTH	CAL	GR- RHOZ	RC	E	1/Q	StK*	EVENT
11710	NORMAL	100-2,6	2,1	1	0,5 0,3 1,2	150	Fractures
11699	NORMAL	200-2,5	2,5	3	12	<150	Fractures
11680	NORMAL	100-2,5	1	<1	1,3 0,5 0,6	152	Lithological Limit
11672	NORMAL	55-2,5	2,0	<1	0,5 1,3 0,5	152	Lithological Limit
11666	WIDENED	150-2,6	2,0	<1	0,5	170	Lithological Limit
11623	WIDENED	50-2,5	1,8	2	0,5 0,5 1,2	150	Lithological Limit
11609	NORMAL	75-2,6	3- 4	5 -6	1,25	160	Fractures
11598	NORMAL	100-2,58	1,7	<1	0,4 0,9 0,4	150	Lithological Limit
11566	NORMAL	100 -2,58	2,2	2,8	0,4 1,8 0,4	150	Fractures
11539	NORMAL	100-2,5	<1	<1	0,2 2 0,2	150	Lithological Limit
11531	NORMAL	160-2,5	2	10	0,2 0,8 0,3	150	Fractures
11526	NORMAL	120-2,5	2	<1	0,4 0,0 1,6	150	Fractures
11512	NORMAL	80-2,5	2	<1	0,2 0,5 0,5	180	Fractures

When the Stonely wave passes in front a fracture applies pressure in the crack pulling fluid inside and decreasing the pressure in the borehole, in consequence the attenuation of the direct wave increases, giving rise to a reflected wave.

The chevron patterns appeared in presence of fractures or interfaces where lithology changes (lithic contact). These points were considered in the Table 1, which contains the depths where chevron patterns were identified, caliper information, Gamma ray and

Density, Reflection Coefficient, Energy in traces[,] tenuation factor, Slowness added by permeability an description of fracture or lithic contact.

Higher peaks of Reflection Coefficients are as[soci]ated to fractures and the lower to lithic contact. Hig[h] reflection coefficients values ($RC > 4$) with high en[ergy] ($E > 5$), abrupt drop in Attenuation factor and hig[h] values in Slowness added by Permeability indicat[e] fracture zone with high permeability located betw[een] 12010 and 12030 feet. This identification coinc[ides]
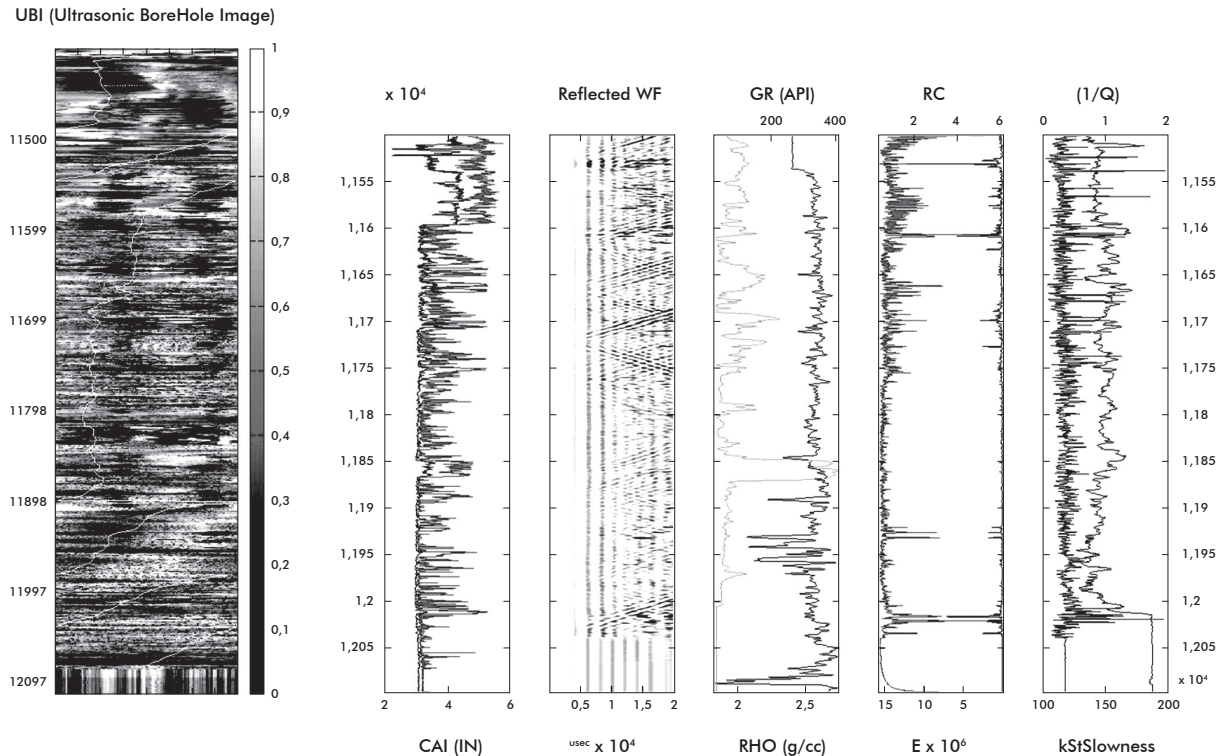
Figure 7 Well total 600 feet (11 500-12 100) with the UBI image information, Caliper, reflected wave, density and Gamma ray, reflection coefficient and energy variation, attenuation and permeability added slowness

with packed of great size fractures that produced 4000 barrels of fluid before be cemented and cased, shown in Figure 8.

Small Reflection Coefficients (*RC < 2*) with small energies (*E ≤ 2*) and rising Attenuation factors were associated to lithic contacts.

Relatively high Reflection Coefficients (*2 < RC < 5*) with moderately high energy (*3 < E < 5*) and mild decreasing Attenuation factors were associated to low quality fractures.

Abnormal behaviors associated to low quality fractures were observed in two intervals. In the 11,932-11,920 feet interval, with high Reflection Coefficients (*2 < RC < 5*) and high energy (*3 < E < 5*) and with decreasing Attenuation factor. The 11 728 - 11 699 feet, with high Reflection Coefficients and high Energy and mild change in Attenuation factor. However, the absence of cores of these intervals impeded to analyze and explain the failures.

5. CONCLUSIONS

- The Stoneley wave approach to detect fractures was imbedded in a program, and applied to a clastic formation in Colombia, providing encouraging results supported by log and core analysis. The software calculated Reflection Coefficient, Energy in traces, Attenuation factor and Slowness added by permeability that used along with borelogs allowed to discriminate fractures and lithic contacts.

- Both high Coefficient Reflection and Energy indicate the presence of fractures, as long as there has been correction for irregularities and changes in lithology, as previously mentioned.

- Changes in the attenuation factor are useful in reconfirming the presence of fractures and contribute in discriminating the effects produced by accentuated lithological limits, as was demonstrated in well logs.
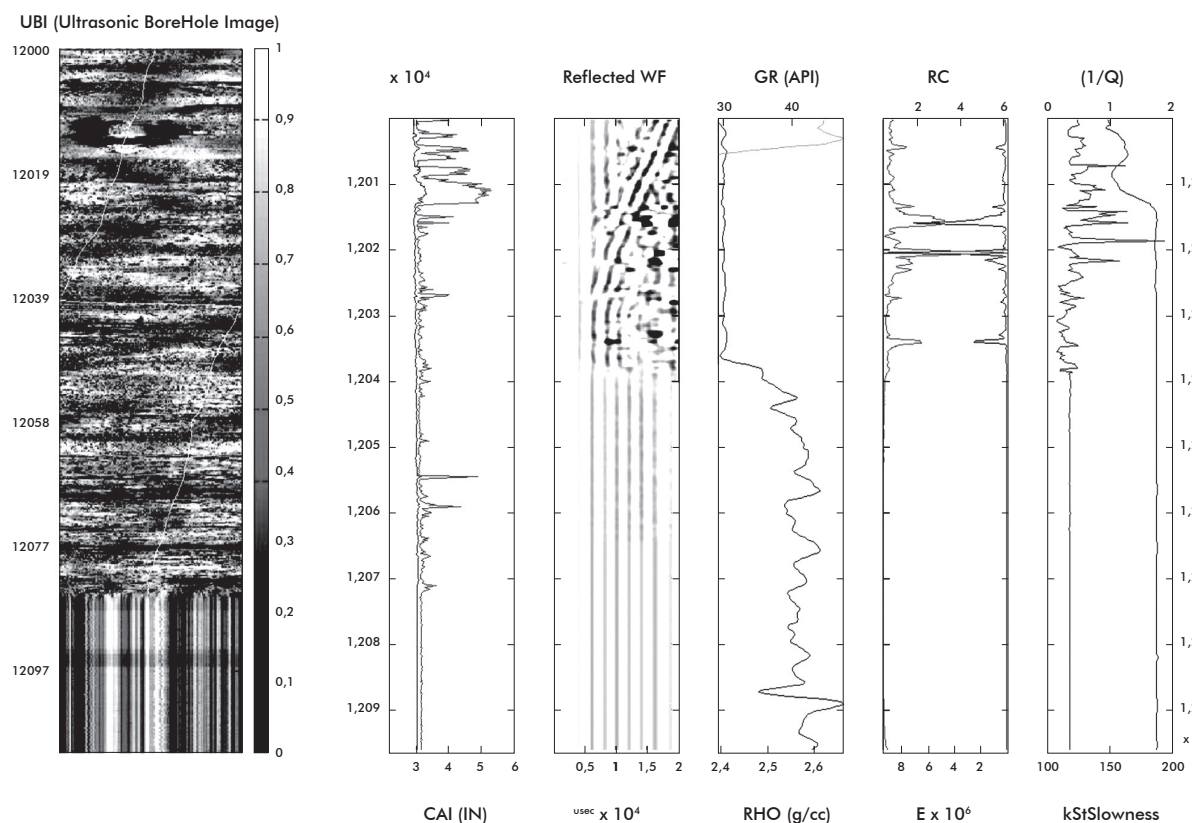
Figure 8 Proven fractured zone (12100-12000) with the UBI image information, Caliper, reflected wave, density and Gamma ray, reflectio[...] coefficient and energy variation, attenuation and permeability added slowness

- The existence of significant permeability in the fracture can be determined by using the Stoneley slowness added by permeability; technique that located a great permeability zone, corroborating its usefulness as a permeability indicator. However, since the density or viscosity of the fluid is not known, it was not possible to calculate the permeability value.

- The lithology and presence of washout and washover in boreholes drilling clastic formations would contribute to explain its low use in Colombia

- The results indicate that the simplified algorithm is effective in detecting fractures with a significant opening and permeability, but not effective in all cases of fissures and is still transparent to the effects of contrast in lithology.

- In spite of promising results, the program could [...] discriminate fractures detected by other techni[...] whence driven research still ongoing.

REFERENCES

Biot, M. A. (1956). Theory of propagation of elastic waves in a fluid saturated porous solid. I. Low frequency range. *J. of Accoustical Soc. of America*, 28, 168-178.

Biot, M. A. (1962). Mechanics of deformation and acoustic propagation in porous media. *J. of Applied Physics*, 33, 1482-1498.

Brown, P., Batzle, M., Dey-Sakar, S., & Peeters, M. (2000). Shock Tube Experiments and observation of the slow Biot wave in natural rocks, *SEG, 70th Annual Conference*. Calgary. 6-11-August.

Chang, S. K., Liu, H. L., & Johnson, D. L. (1988). Low frequency tube waves in permeable rocks, *Geophysics*, 53, 519-527.

Cheng-Chuen, & Toksoz, M. (1981). Elastic wave propagation in a fluid filled borehole and synthetic acoustic logs, *Geophysics*, 46, 1042-1053.

Cheng, C. H., Zhang, J., & Burns, D. R. (1987). Effects of in situ permeability on the propagation of Stoneley wave in a borehole, *Geophysics*, 52, 1279-1289.

Endo, T., Ito, H., Brie, A., Badri, M., & El Sheikh, M. (1997). Fracture and permeability evaluation in a fault zone from sonic waveform data, in Transactions of the SPWLA (Society of Professional Well Log Analysts). *Paper R. 13*. Thirty-Eighth Annual Logging Symposium, ouston, Tex.: Society of Professional Well Log Analysts, June 15-18.

Hornby, B. E., Johnson, D. L., Winkler, K. W., & Plumb, R. A., (1989). Fracture evaluation using reflected Stoneley wave arrivals, *Geophysics*, 54, 1274-1289.

Kosteck ,S., Jonson, D. L.. Kenneth W. W., & Hormby, Br. (1988). The interaction of tube waves with borehole fractures. Part I: Numerical Models. *Geophysics,* 63, 800-808.

Latifa, Q., Tang X. M., & Kuijperl, A. (2001). Permeability determination from Stoneley waves in the Ara group carbonates, Oman. *GeoArabia* 6 (4): 649-666.

Paillet, F. L. & White, J. E. (1984). Acoustic modes of propagation in the borehole and their relationship to rock properties, *Geophysics,* 47, 1215-1228.

Rosenbaum, J. H. (1974). Synthetic micro seismograms: logging in porous formation: *Geophyisics*, 39, 14-39.

Tezuka, K., Endo, T., Miyairi, A., & Brie, H. (1995). Fast Stoneley modeling and its application for permeability fracture evaluation. *Paper of First annual well logging symposium of Japan*. Chiba, September 21-22.

Tezuka, K., & Cheng, C. H. (1997). Modeling of low frequency Stoneley wave propagation in irregular borehole. *Geophysics*, 62, 1047-1058.

Williams, D. M., Zemanek, J., Angona, F. A, Denis, C. L., & Caldwell, R. L. (1984). Society of Professional Well Log Analysts Annual Logging Symposium 25th, New Orleans. *Transactions*. p. T1-T16.

Wisse, C. J., Smeulders, D. M. J., & Dongen, M. E. H. (1998). Shock tube measurements on water-saturated porous cylinders, *Paper presented at the 4th Biot Conference* on Poromechanics, Louvain-la-Neuve, Belgium, September 14-16.

APENDIX

Data Structure

    The entry data are three matrixes in three files in ".las" format, whose structure is described below:

UBI (Ultrasonic Borehole Imager)	(Matrix 1)
NAME	DESCRIPTION
Dept.	Column depth
AWBK[0…139]	Wave attenuation amplitude
UPAZ	Corrected UBI azimuth
P1AZ	Pad 1 Azimuth
DSI (Dipolar Shear Imager)	**(Matrix 2)**
NAME	DESCRIPTION
Dept.	Column depth
PWF3 [0….512] and [0…4097]	Packed waves
DTST	Delta T Stoneley
DT4S	Delta T Shear
DT4P	Delta T Compressional
CFVL	Fluid Velocity
RCAV	Corrected radius Average
RCMX	Corrected radius Maximum
RCMN	Corrected Radius Minimum
BS	Bit Size
Additional Data Logs	**(Matrix 3)**
NAME	DESCRIPTION
RHOZ	Formation Density
GR	Gamma Ray
NPHI	Neutron Porosity
POTA	Potassium Contents
THOR	Thorium Contents
URAN	Uranium Contents